Inversion for the Velocity Field in the Solar Interior

Jesper Schou

Stanford University, HEPL Annex A201, Stanford, CA 94305-4085, USA

1 Introduction

The Sun is oscillating in a large number of normal modes. Most of the modes observed are acoustic waves, but surface gravity modes are also observed. These modes are described by 3 'quantum' numbers: the radial order n, the degree l and the azimuthal order m, with $|m| \leq l$. The angular dependence of the mode eigenfunctions is determined by l and m, while the radial dependence is determined by n and l. If the Sun were spherically symmetric the mode frequencies $\omega_{nlm} = 2\pi\nu_{nlm}$ would not depend on m. Asphericities such as rotation lift this degeneracy. Modes have been observed with l from 0 to several thousand, n from 0 to about 40 and frequencies between $\approx 1mHz$ and $\approx 10mHz$ with a peak at $\nu \approx 3mHz$. The modes have been observed with several different instruments. Most instruments are only able to observe a limited range of l and have observed for a limited time. In the future we expect high quality observations over a large range of l for long periods from instruments such as GONG (a ground based network) and SOI/MDI on the SOHO spacecraft launched in 1995.

Here I shall describe how inverse methods have been used to infer the rotation rate in the solar interior from mode frequencies.

2 The Forward Problem

The frequency shift caused by rotation is given by

$$2\pi\Delta\nu_{nlm} = \Delta\omega_{nlm} = \omega_{nlm} - \omega_{nl} = \int_0^\pi \int_0^1 K_{nlm}(r,\theta)\Omega(r,\theta) r dr d\theta \qquad (1)$$

where r is the fractional radius, θ is the co-latitude, ω_{nl} is the unperturbed mode frequency and K_{nlm} is an (assumed) known non-negative function which can be found as described in Schou et al. 1994. For high-l

$$K_{nlm}(r,\theta) \simeq m P_l^m(\cos\theta)^2 \sin\theta \rho(r) r I_{nl}^{-1} \left(\xi_{nl}(r)^2 + \eta_{nl}(r)^2\right) \ , \qquad (2)$$

where P_l^m is an associated Legendre function and I_{nl} a normalization factor. Examples of the radial and latitude dependence are shown in Fig. 1, as can be

seen the kernels vanish rapidly below the so-called radial turning point r_t and below the turning point in co-latitude θ_t and are oscillatory above these points.

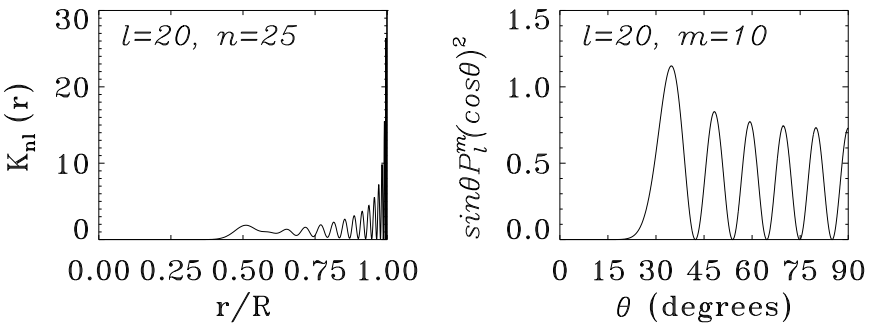

Fig. 1. Examples of kernels given by Eq. 2. The left plot shows an exact latitude averaged kernel used in Eq. 1. The right plot shows an example of $\sin\theta P_l^m(\cos\theta)^2$.

3 Solution of the Inverse Problem

In the 1D case (latitude independent rotation) the number of splittings is of the order a few thousand and the kernels can be described adequately using a discretization with, say 1000 points. These low numbers make it possible to use a number of inversion methods such as regularized least squares (RLS), Backus-Gilbert (known as (subtractive/multiplicative) optimally localized averages) and asymptotic methods. In the 2D case, the number of splittings is of the order 10^5 to 10^6 and the necessary number of mesh points is of the order 10^5. This and the fact that the problem can not be separated in radius and latitude means that a brute force implementation of most of the 1D methods is not feasible.

At least 3 different methods have been used for the 2D case:
1. Expand the latitude dependence of Ω in polynomials in $x = \cos\theta$ and the m dependence of the splittings in polynomials in m. These methods have been dubbed 1.5-dimensional methods (Brown, et al. 1989, Schou, et al. 1994).
2. So-called $1\otimes1$ methods (Sekii 1993) in which one separates radius and latitude in a way similar to Eq. 2.
3. A full two dimensional RLS inversion. (Schou et al., 1994.)

I will briefly describe method 3. In the current implementation we minimize

$$\sum_i \left(\frac{\int K_i\bar\Omega r\mathrm{d}r\mathrm{d}\theta - \Delta\omega_i}{\sigma_i}\right)^2 + \mu_r\int\left(\frac{\partial^2\bar\Omega}{\partial r^2}\right)^2 f_r\mathrm{d}\theta\mathrm{d}r + \mu_\theta\int\left(\frac{\partial^2\bar\Omega}{\partial\theta^2}\right)^2 f_\theta\mathrm{d}\theta\mathrm{d}r\ , \tag{3}$$

here i stands for the combination nlm; σ_i is the standard deviation of $\Delta\omega_i$, $\bar\Omega$ is the inferred rotation rate, μ_r and μ_θ are trade-off parameters and f_r and f_θ are (non-negative) weight functions. The rotation rate is described as a bilinear

function on a rectangular grid. Unfortunately it is not feasible to use a sufficient number of points to adequately resolve the kernels in both radius and latitude. Our solution to this problem has been to use a fine grid for calculating the integrals of the basis functions with the kernels and a coarser grid for the solution. The effect of the inadequate resolution is to add another regularization term to Eq. 3. So far, however, the signal to noise ratio has not been high enough to make use of the potential resolution of the kernels.

The choice of the trade-off parameters and weight functions determines the trade-off between the resolution and the effects of input errors on the inferred rotation rate. For the results shown here f_r has been chosen to be proportional to r and f_θ to be proportional to r^{-4}. I will not discuss how to choose the trade-off parameters in this poster. In addition to changing the regularization parameters it is possible to use other functional forms for the regularization such as first derivatives or mixed terms in radius and latitude.

Figure 2a shows a rotation rate used for generating artificial data. An inversion of data generated using this rotation rate is shown in Figs. 2b and 2c. The modeset used had modes with $1 \leq l \leq 200$ and frequencies between $1mHz$ and $4mHz$ representing what we expect to have in the near future from the GONG project. The errors were estimated theoretically assuming 1 year of continuous observations. This modeset had 153217 splittings and we used 50 intervals in radius and 24 in latitude to describe the inferred rotation rate (we have used more than twice the number of points in each direction for some inversions).

The difference between Figs. 2b and 2c indicates the magnitude of the errors, which have not been shown separately. These errors only represent the effect of the errors on the input splittings, they are *not* an estimate of the difference between the true and inferred rotation rates, which can be substantially larger due to rapid unresolved variations in the true rotation rate. Also the errors on different points of the inferred rotation rate can be highly correlated, which is generally ignored (see, however, Schou 1991).

As in any linear inversion method *averaging kernels* $\mathcal{K}$ exist such that

$$\bar{\Omega}(r_0, \theta_0) = \int_0^R \int_0^\pi \mathcal{K}(r_0, \theta_0; r, \theta) \Omega(r, \theta) r \mathrm{d}r \mathrm{d}\theta \ , \tag{4}$$

plus an error term. These averaging kernels (the resolution matrix) describes how the inferred rotation rate is actually a weighted integral of the true rotation rate. Examples are shown in Fig. 2d.

4 Some Real Results

The result of an inversion of a real dataset is shown in Fig. 3. These results are from an instrument called LOWL (Tomczyk 1995), designed to cover all l's from 0 to 80. Most earlier instruments have not been able to cover both the lowest l's and higher l's, making it necessary to combine different datasets (possibly leading to systematic errors) to infer the rotation rate in the solar core. The inversion shown here used 2119 'splittings' from 716 (n, l) multiplets. Instead of using real

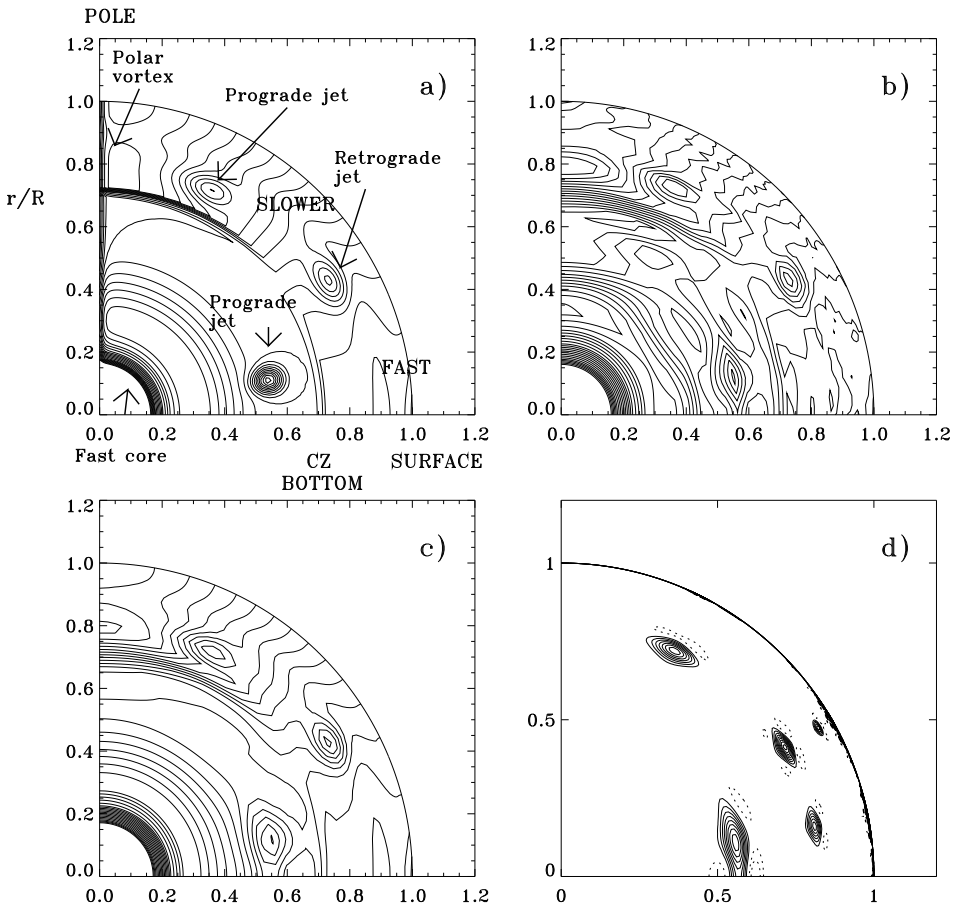

Fig. 2. (*a*) Artificial rotation profile. (*b*) Recovered solution with data containing random noise appropriate to one year's observations. (*c*) Recovered solution for noise-free data, but with the same data uncertainties assumed as for *b*. In *a*–*c*, the contour spacing is 10 nHz. (*d*) Averaging kernels at different target radii and latitudes. Solid contours are positive, broken contours are negative. For clarity the zero contour is omitted.

splittings the variation of mode frequency with m was expanded in polynomials and the inversion was performed using the coefficients in the polynomial fits. These results are in general agreement with those found previously, except that they go down to 0.2 unlike most earlier inversions which only went to 0.4.

The most notable features of the inferred rotation rate are the near discontinuity at the bottom of the convection zone (at ≈ 0.7) and a lack of significant radial variation of the rotation rate in the convection zone which is in sharp contrast to the results expected theoretically. In the radiative interior below the convection zone the Sun appears to rotate as a solid body.

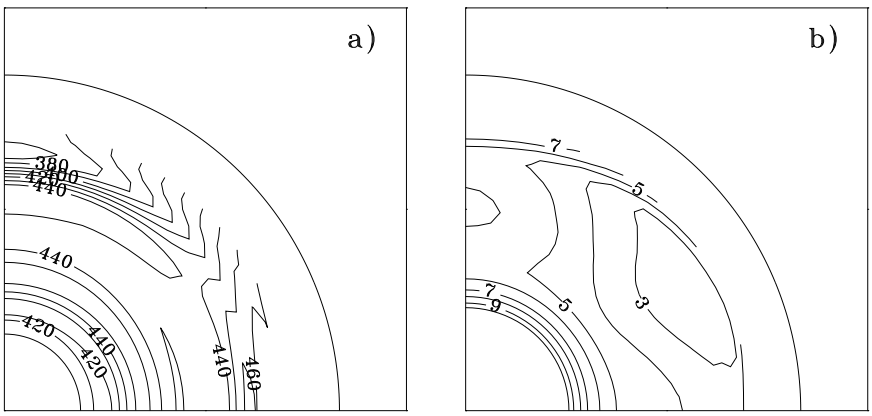

Fig. 3. (a) The solar rotation rate between $r = 0.2R_\odot$ and $r = 0.85R_\odot$, as inferred using the 2D RLS technique with $\mu_r = 10^{-7}$, $\mu_\theta = 10^{-3}$. The contour spacing is 10 nHz. (b) The corresponding 1-σ error levels (values are in nHz).

5 Discussion

As mentioned earlier the kernels K_{nlm} are assumed known. Fortunately the main effect of the uncertainties in the solar structure, from which the kernels are calculated, is to distort the radial scale slightly, which is fairly harmless.

Correlated errors are also a problem. Unfortunately little has been done to estimate the magnitude of the off diagonal elements of the covariance matrix (see Schou, et al. 1995 for some estimates) or their effect on the inversions.

The method described here is, as mentioned, only one of several that have been applied to helioseismic data and the estimation of the rotation rate is only one of several properties that have been investigated using inverse methods. Most of the methods applied have been rather 'traditional' in the sense that they have been RLS or Backus-Gilbert like. This has been due to a combination of computational problems, lack of good constraints (prior information) to apply and limited data quality. Some attempts to set bounds on the pointwise values of the rotation rate or certain averages have also been made. In particular the robustness of the conclusion that the rotation rate in the solar convection zone is constant on radii and that the latitude gradient disappears at the bottom of the convection zone has been the subject of several studies. (eg. Gough, et al. 1993, Schou and Brown 1994, and Genovese et al. 1995). A problem has been that we do not have tight limits on the rotational velocities based on physical considerations. Among the constraints imposed have been that the rotation speed should be less than the speed of light and (less strict) that the matter should be gravitationally bound. Another problem has been the expansion of the mode frequencies in polynomials which turns out to significantly limit how tightly the rotation rate can be constrained. In the future we expect to have significantly

more terms in the polynomials or individual frequency splittings.

We are also working on developing other inversion methods and improving on the speed of some of the presently used methods. Despite the simplifications already made the algorithms are extremely memory and cpu time intensive. We are looking in to such options as preprocessing the data and using more complex discretizations than a rectangular grid.

When a new generation of instruments such as GONG and SOI/MDI start producing data we expect to obtain significantly more accurate splitting measurements over a substantial range in l and frequency, thereby vastly improving our knowledge of the solar interior.

A substantial part of the work described in this poster was done in collaboration with a number of people, in particular Jørgen Christensen-Dalsgaard, Mike Thompson and Steve Tomczyk.

References

Brown, T. M., Christensen-Dalsgaard, J., Dziembowski, W. A., Goode, P., Gough, D. O. and Morrow, C. A., 1989. Inferring the Sun's Internal Angular Velocity from Observed p-Mode Frequency Splittings. Astrophysical Journal, 343, 526-546.

Genovese, C. R., Stark, P. B. and Thompson, M. J., 1995. Uncertainties for Two-Dimensional Models of Solar Rotation from Helioseismic Eigenfrequency Splitting. Astrophysical Journal, 443, 843-854.

Gough, D. O., Kosovichev, A. G., Sekii, T., Libbrecht, K. G., and Woodard, M. R. 1993. The Form of the Angular Velocity in the Solar Convection Zone. In: T. M. Brown (ed.), GONG 1992: Seismic Investigation of the Sun and Stars, Astronomical Society of the Pacific Conference Series, Volume 42, San Francisco, 213.

Schou, J., 1991. On the 2-Dimensional Rotational Inversion Problem. In: D. Gough and J. Toomre (eds.), Challenges to Theories of the Structure of Moderate-Mass Stars, Lecture Notes in Physics volume 388, Springer-Verlag, Berlin, 93-100.

Schou, J. and Brown, T. M., 1994. On the Rotation Rate in the Solar Convection Zone. Astrophysical Journal, 434, 378-383.

Schou, J., Christensen-Dalsgaard, J. and Thompson, M. J., 1994. On Comparing Helioseismic Two-Dimensional Inversion Methods. Astrophysical Journal, 433, 389-416.

Schou, J., Christensen-Dalsgaard, J. and Thompson, M. J., 1995. Some Aspects of Helioseismic Time-Series Analysis. In: R. K. Ulrich, E. J. Rhodes, Jr. and W. Däppen (eds.), GONG '94: Helio- and Astero-Seismology From the Earth and Space, Astronomical Society of the Pacific Conference Series, Volume 76, San Francisco, 528-531.

Sekii, T., 1993. On an $1 \otimes 1$ Inversion Technique for Solar Rotation. In: T. M. Brown (ed.), GONG 1992: Seismic Investigation of the Sun and Stars, Astronomical Society of the Pacific Conference Series, Volume 42, San Francisco, 237-240.

Tomczyk, S., Streander, K., Card, G., Elmore, D., Hull, H. and Cacciani, A., 1995. An Instrument to Observe Low-Degree Solar Oscillations. Solar Physics, 159, 1-21.

This article was processed using the LaTeX macro package with LMAMULT style